Tunnelling through moving barriers

1991 J. Phys. A: Math. Gen. 24 3533

(http://iopscience.iop.org/0305-4470/24/15/021)

J. Phys. A: Math. Gen. 24 (1991) 3533-3550. Printed in the UK

Tunnelling through moving barriers

A Pimpale†, S Holloway‡ and R J Smith‡

† Department of Physics, University of Poona, Ganeshkhind, Pune 411 007, India
‡ Surface Science Research Centre and Department of Chemistry, University of Liverpool, PO Box 147, Liverpool L69 3BX, UK

Received 17 January 1991

Abstract. In this paper we present a variety of theoretical methods to treat the general problem of a quantum particle interacting with a time-dependent barrier. Assuming a sinusoidal form for the time dependence, we discuss the classical, semiclassical and quantum solutions for two specific problems: a barrier whose amplitude is modulated, and one whose mean position changes. While the classical solutions to these problems are quite different, the time-independent quantum solutions appear almost identical. It is only when the particle is modelled as a wavepacket that the quantum solutions behave like their classical counterparts.

1. Introduction

Tunnelling is a basic quantum mechanical phenomenon with many interesting applications [1]. Time-dependent barriers appear in the tunnelling context in two different physical situations. First, when an incident particle loses or gains energy in the tunnelling process the situation can be described in the language of inelastic scattering and non-conservation of particle energy can be modelled by a time-dependent potential barrier. If the potential has a time modulated term of the form $V(x)\cos\omega t$, then the particle energy changes by discrete quanta of frequency ω, i.e., by energy $n\hbar\omega$. Büttiker and Landauer [2, 3] have studied this problem at some length, with an aim to identify the tunnelling traversal time, a problem having a rich history [4, 5]. They explicitly evaluated the strength of the $\pm\hbar\omega$ sidebands in the limit of a weak harmonic perturbation and from these intensities defined a tunnelling time. Their formalism has recently been used and further developed by other workers [6].

Secondly, in many chemical reactions involving hydrogen, particularly at surfaces, the bond breaking and making process is often described by a particle tunnelling through a region of the potential energy hypersurface [7]. In this case, the potential barrier has its origins in the electronic interaction between the gas atom and those atoms comprising the surface. These surface atoms are not stationary but undergo oscillations, either due to zero-point motion or corresponding to their excited states, and therefore the potential barrier has a time dependence, in amplitude and position, which is characterized by a surface vibrational frequency. The problem is also of an intrinsic interest as it corresponds to solving a parabolic partial differential equation subject to space-time-dependent boundary conditions.

In this paper we consider a general theory of tunnelling through time-dependent potential barriers, particularly with an oscillatory time dependence which is confined to a finite spatial region. The development of the paper is as follows. In section 2 we

0305-4470/91/153533+18$03.50

consider the problem classically and compare and contrast an oscillating amplitude with a spatially oscillating rectangular potential barrier. Classically, the two barriers behave in different ways, in the former case there being no change in the particle energy as it is reflected by the barrier, whereas for a spatially oscillating barrier the particle energy changes due to collision with the moving barrier, the energy change being dependent upon the exact time of collision. In section 3 we formulate the problem quantum mechanically and show that for both kinds of time dependence the quantum situation is similar in contradistinction to the classical case. The oscillating rectangular barrier is then discussed in detail in section 4 and it is shown that the transmission and reflection coefficients are independent of the choice of time origin (i.e. the phase of the oscillating potential) although the details of the wavefunction in the barrier region are dependent on it. Some exact numerical calculations are presented in section 5 and conclusions are summarized in section 6. An appendix is devoted to approximate analytical approaches for solving the time-dependent Schrödinger equation in the presence of an oscillating potential.

Throughout this paper we have considered only one spatial dimension.

2. Classical modelling

The classical motion of particle is governed by the local equations of motion. If the time-dependent potential is confined to a finite spatial region, say $\mathfrak{R}$, away from this region a local constant of motion, energy, can be defined. If the initial conditions are such that the particle always remains outside $\mathfrak{R}$, the time-dependent potential has no effect on such solutions of the equations of motion. However, when the particle trajectory approaches $\mathfrak{R}$ and enters it, the motion is affected. Eventually, the particle may emerge from $\mathfrak{R}$ with, in general, a different energy which is not uniquely defined in terms of the initial energy, being also dependent upon the choice of time-origin. When the time-dependence is oscillatory one can average over the choice of the time-origin in one time period. We now consider two simple models of rectangular barriers with sinusoidal time-dependences.

2.1. The oscillating amplitude barrier

This model is described by a potential

$$V(x,t)=\begin{cases} V_0+V_1\cos(\omega t+\phi) & 0\leqslant x\leqslant a \\ 0 & x<0 \text{ and } x>a \end{cases} \tag{1}$$

where $V_0>V_1$ are assumed positive. A particle of energy $0<E<V_0-V_1$ is confined either to the left or to the right of the barrier for all initial conditions and choices of time-origin (i.e. value of ϕ). When $E>V_0+V_1$ classical motion is permissible over the entire real line. Assuming that the particle of energy E comes from the left at $x=0$ at $t=0$, it will emerge at $x=a$ at time T with energy $E+V_1\{\cos(\omega T+\phi)-\cos\phi\}$, where T is given by $a/\sqrt{2(E-V_0-V_1\cos\phi)/m}$, m being the mass of the particle. Thus the energy of the particle can vary between $E-2V_1$ to $E+2V_1$ for appropriate values of T and ϕ. When the initial energy $V_0-V_1<E<V_0+V_1$, the particle will be reflected for some values of ϕ but traverse the barrier for other values of ϕ. In all cases there is no change in particle energy when it is reflected at the barrier, and following traversal the energy change corresponds to the barrier height at the instant of crossover.

2.2. Oscillating position potential

This potential is given by

$$V(x, t) = U(x - \alpha \cos(\omega t + \phi)) \tag{2}$$

where $U(x)$ is a rectangular barrier of height V_0 and width a:

$$U(x) = V_0[\theta(x) - \theta(x-a)] = \begin{cases} V_0 & 0 \leqslant x \leqslant a \\ 0 & \text{otherwise.} \end{cases} \tag{3}$$

The region $\Re$ now is time-dependent and extends from $\alpha \cos(\omega t + \phi)$ to $\{a + \alpha \cos(\omega t + \phi)\}$.

Consider a particle of energy E and velocity $\dot{x} > 0$ incident from left of the barrier. Without loss of generality, we choose the time origin such that the particle is at $x = -\alpha$ at $t = 0$. Let the particle encounter the barrier at $t = T > 0$ given by

$$-\alpha + \dot{x}_0 T = \alpha \cos(\omega T + \phi). \tag{4}$$

The velocity of the barrier at this instant is

$$v_b = -\alpha\omega \sin(\omega T + \phi) \tag{5}$$

and the relative energy of motion between the particle and the barrier is

$$E_{\mathrm{Rd}} = \tfrac{1}{2} m(\dot{x}_0 - v_b)^2. \tag{6}$$

The particle is reflected at the barrier if $E_{\mathrm{Rd}} < V_0$ and it crosses over the barrier if $E_{\mathrm{Rd}} > V_0$. Note that unlike the oscillating amplitude case, for sufficiently high frequency ω, one can always have $E_{\mathrm{Rd}} > V_0$. Also, when the particle is reflected, it suffers a change in laboratory kinetic energy given by

$$\Delta E = \tfrac{1}{2} m\{(-\dot{x}_0 + 2v_b)^2 - \dot{x}_0^2\} = 2mv_b(v_b - \dot{x}_0). \tag{7}$$

When $E_{\mathrm{Rd}} > V_0$ and the particle enters the region $\Re$, the relative velocity v_{Rd} between the particle and the barrier is given by

$$\tfrac{1}{2} m v_{\mathrm{Rd}}^2 = E_{\mathrm{Rd}} - V_0 \qquad V_{\mathrm{Rd}} > 0 \tag{8}$$

and the velocity of the particle in the laboratory is

$$\dot{x}(t > T) \equiv \dot{x}_1 = v_{\mathrm{Rd}} - v_b. \tag{9}$$

The particle moves inside $\Re$ with constant velocity $\dot{x}_1$, until it collides with either the left or the right wall of the barrier at time, say, T_1 or $T_1' > T$ given by

$$-\alpha + \dot{x}_0 T + \dot{x}_1 T_1 = \alpha \cos(\omega T + \omega T_1 + \phi)$$

for collision with the left wall or

$$-\alpha + \dot{x}_0 T + \dot{x}_1 T_1' = a + \alpha \cos(\omega T + \omega T_1' + \phi)$$

for collision with the right wall, whichever comes first. The particle then emerges from the region $\Re$ with changed energy due to the potential step V_0 as well as the relative time-dependent velocity at the instant T_1 or T_1'. The situation is depicted schematically in figure 1.

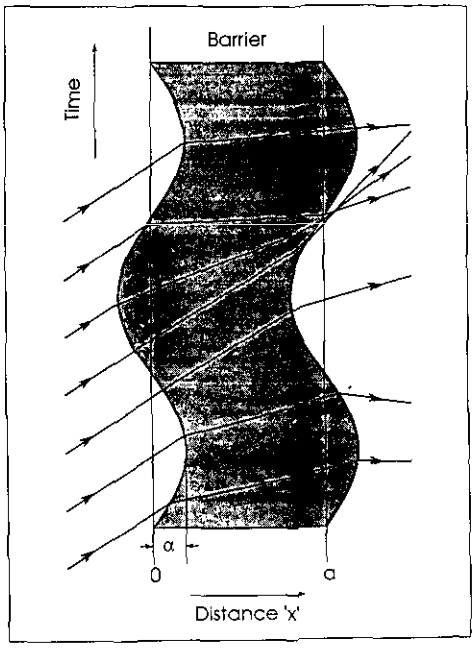

Figure 1. Schematic classical trajectories for a particle in an oscillating rectangular potential barrier for different phases ϕ.

3. Quantum mechanical formulation

The time evolution of the wavefunction is governed by the Schrödinger equation

$$i\hbar \frac{\partial \psi(x, t)}{\partial t} = \mathcal{H}\psi(x, t) \tag{10}$$

where the Hamiltonian operator is

$$\mathcal{H}(x, t) = \frac{-\hbar^2}{2m} \frac{\partial^2}{\partial x^2} + V(x, t).$$

When the potential is an oscillatory function of time with a period $2\pi/\omega$, the Schrödinger equation is invariant under the transformation

$$t \to t + \frac{2\pi}{\omega}. \tag{11}$$

Applying Floquet's theorem [8], the wavefunction has the form

$$\psi(x, t) = \exp(\mathrm{i}\nu t)\Phi(x, t) \tag{12}$$

where ν is a constant and Φ has the periodicity of the potential

$$\Phi(x, t + 2\pi/\omega) = \Phi(x, t). \tag{13}$$

Expanding Φ in a Fourier series we get

$$\psi(x, t) = \sum_{n=-\infty}^{\infty} \exp[\mathrm{i}(\nu + n\omega)t] F_n(x) \tag{14}$$

where the F_n are the various Fourier coefficients. Noting that $i\hbar\partial/\partial t$ is the energy operator, then the nth term in (14) corresponds to an energy of $\hbar\nu + n\hbar\omega$. One can qualitatively interpret (14) as a particle with an initial energy $E = \hbar\nu$ developing an energy spread due to interaction with the time-dependent potential.

For the oscillating amplitude potential of (1), the Schrödinger equation can be explicitly solved [2]. The solution is given by (14) with

$$F_n(x) = \exp(ipx/\hbar) J_n(V_1/\hbar\omega) \qquad \begin{cases} x > a \\ x < 0 \end{cases} \tag{15}$$

where $p^2/2m = \hbar\nu \equiv E$ and J_n are the Bessell coefficients. In (15) the phase factor ϕ is omitted for simplicity.

We now consider time-dependent potentials of the form

$$V(x, t) = U(x - g(t)). \tag{16}$$

For oscillatory potentials of the above form

$$g(t) = g(t + 2\pi/\omega)$$

and for sinusoidal time-dependence as in (2)

$$g(t) = \alpha \cos(\omega t + \phi). \tag{17}$$

It is convenient to make a non-Galilean transformation to a moving coordinate frame:

$$x \to x' = x - g(t) \tag{18a}$$

$$t \to t' = t \tag{18b}$$

$$\psi \to \psi' = \psi(x', t'). \tag{18c}$$

Dropping the primes for simplicity, (10) then becomes

$$\left[-\frac{\hbar^2}{2m} \frac{\partial^2}{\partial x^2} + U(x) \right] \psi(x, t) = i\hbar \frac{\partial \psi}{\partial t} - i\hbar f(t) \frac{\partial \psi}{\partial x} \tag{19}$$

where

$$f(t) = dg(t)/dt \equiv \dot{g}. \tag{19a}$$

Equation (19) could be rewritten as

$$\left[\frac{1}{2m} \left(-i\hbar \frac{\partial}{\partial x} - mf \right)^2 + U \right] \psi = \left[i\hbar \frac{\partial}{\partial t} + \tfrac{1}{2} mf^2 \right] \psi. \tag{20}$$

The usual quantum identification of momentum and energy in the moving frame as $-i\hbar\partial/\partial x$ and $i\hbar\partial/\partial t$ in (20) gives us back the energy-momentum dispersion relation.

We next consider an application of (18).

4. Tunnelling through an oscillating potential: exact solution

Equation 18 can be solved exactly for the oscillating position potential of (3) in different spatial regions. The solution is of the form

$$\psi(x, t) = \exp(ipx/\hbar) \exp\left[-\frac{i}{\hbar} (Et - pg(t)) \right] \qquad x > a, x < 0 \tag{21}$$

where

$$p^2/2m = E \tag{22}$$

Using (17) for $g(t)$ and Fourier expanding (21) we recover (14) for the wavefunction, with the Fourier coefficients given by (15). Thus although classically the two models of sections 2.1 and 2.2 are quite different, quantum mechanically they are rather similar.

For $P > 0$, (21) represents a wave moving from left to right. Considering a reflected wave at the boundary $x = 0$ and a transmitted wave for $x > a$, the wavefunction in different regions can be written as

$$\psi(x, t) = \exp\left(\frac{-iEt}{\hbar}\right) \times \begin{cases} \exp[ip(x+g(t))/\hbar] + R\exp[-ip(x+g(t))/\hbar] & (x<a) \\ A\exp[iq(x+g(t))/\hbar] + B\exp[-iq(x+g(t))/\hbar] & (0<x<a) \\ T\exp[ip(x+g(t))/\hbar] & (x>a) \end{cases} \tag{23}$$

where $g(t)$ is given by (17) and

$$q^2/2m + V_0 = E. \tag{24}$$

In the tunnelling context, $E < V_0$ and q is pure imaginary.

It is not possible to apply the wavefunction continuity conditions at $x = 0$ and $x = a$ for all times to get the constants R, A, B and T. However, it is possible to write down these conditions at a particular instant, say $t = 0$. We then get four linear inhomogeneous equations for the four constants which are dependent upon the choice of time-origin through the arbitrary phase ϕ. It is straightforward to solve these equations for the reflection and transmission coefficients R and T:

$$R = 2i\exp[ip(a + 2\alpha\cos\phi)](p^2 - q^2)\sin(qa)/D \tag{25}$$

and

$$T = -4pq/D \tag{26}$$

with the denominator D given by

$$D = -\exp(-ipa)[4pq\cos(qa) - 2i(p^2 + q^2)\sin(qa)]. \tag{27}$$

In (25) and (27) we have set $\hbar = 1$ for simplicity.

It is interesting to note that the transmission coefficient T is independent of the phase ϕ and thus insensitive to the choice of time-origin. This situation has been observed earlier by Büttiker and Landauer [3] but is shown here explicitly for the first time. Since p is real, the reflection coefficient R depends upon ϕ only through a phase factor. The coefficients A and B giving the wavefunction inside the barrier are more complicated function of ϕ. It is readily seen that

$$|R|^2 + |T|^2 = 1. \tag{28}$$

Equation 28 is really a consequence of Hermiticity of the Hamiltonian which is not affected by the time-dependence of the potential.

5. Numerical results

We now consider the problem of a Gaussian wavepacket incident upon a time dependent barrier. For simplicity again only one spatial dimension will be studied. This sort of problem has been studied on many occasions in connection with the definition of the 'correct' procedure for calculating the tunnelling time [9]. Although this is a worthy debate, we prefer not to be drawn into this discussion but instead will investigate how the tunnelling probability is connected with the two timescales (i) the round-trip of the scattered particle and (ii) the period of the barrier oscillation.

5.1. The oscillating position barrier

Specifically we consider an electron scattered by a Gaussian shaped barrier which falls into the class given by (2), namely an oscillating hat potential,

$$V(x, t) = V_0 \exp\{-\sigma[x-(x_0+A\sin(\omega t+\phi))]^2\}. \tag{29}$$

For all that follows the height of the barrier, V_0 is 200 au and the width parameter, σ is 1.0 au. The electron energy, ε, the amplitude, A, and frequency, ω will be the subject of the investigation. The initial wavepacket is given by

$$g(x-x_i, p_x) = \frac{1}{\sqrt[4]{2\pi\delta^2}} \exp\{[-(x-x_i)^2/4\delta^2 - ip_x x]\} \tag{30}$$

where x_i is its initial position, p_x its momentum and δ its width. δ was chosen to be 0.5 au which is an optimized value to give the packet a relatively narrow energy spread while still fitting in a box of length 15 au. To solve the time-dependent Schrödinger equation, equation 10, the split operator method of Feit *et al* [10] has been employed. This method has been applied many times to surface scattering problems of this kind and for details the interested reader is referred to literature [11–13]. It need only be mentioned that the method is particularly efficient and is norm conserving.

Figure 2 shows the behaviour of the tunnelling probability as a function of the initial electron energy, $T(\varepsilon)$, for three different values of the barrier frequency

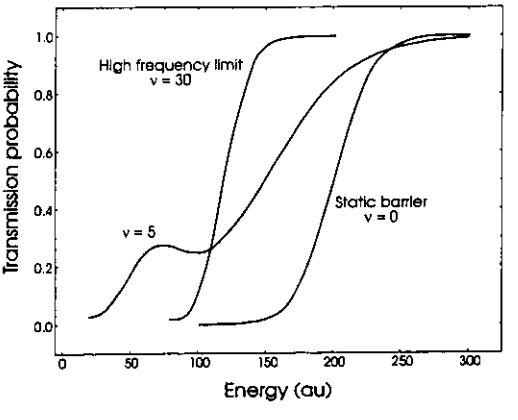

Figure 2. Transmission probability for a particle incident on an oscillating position barrier as a function of the initial translational energy. Results are presented for both high ($\nu = 30$) and low ($\nu = 0$) frequency limits as well as a representative phase ($\phi = 0$) at an intermediate value ($\nu = 5$). For this case, the particle interaction time and the barrier period are similar resulting in an interaction which depends markedly on the initial phase of the barrier.

$\nu(=\omega/2\pi)$ when the amplitude of oscillation is 0.5 au. To set a time scale, the duration for the packet to make a round trip at an energy of 150 is ~1.711 atomic time units. The static barrier represents the low frequency limit and has a well known sigmoidal dependence for $T(\varepsilon)$ which can be found in any elementary quantum mechanics text book [14]. It is a general result that for barriers which are not discontinuous, the tunnelling probability is approximately 0.5 at the energy corresponding to the barrier height. This is indeed the case here and the results are in good agreement with those obtained from a time-independent calculation.

When $\nu = 30$ oscillations per atomic time unit, then the high frequency limit has been reached and increasing ν causes no change to $T(\varepsilon)$, results are also independent of the initial phase of the barrier, ϕ. There is a marked shift in the tunnelling to lower energies, implying that the barrier motion serves to reduce the barrier height. This is simple to understand on the basis of a time-independent potential defined by

$$V(x) = \frac{1}{\tau}\int_0^\tau \mathrm{d}t\, V(x, t). \tag{31}$$

Figure 3 shows $V(x)$ for a range of different values of A. The barrier becomes smeared out in the x coordinate and is significantly reduced in energy. If the amplitude is in excess of 0.5 au then $V(x)$ begins to have a bimodal structure which is an indication that the turning points are sampled preferentially in the average of (31). The rule of thumb mentioned above appears to hold in that 50% tunnelling probability occurs at the value of ~125 au, as seen in the effective potential corresponding to $A = 0.5$ au. It is also clear that the $\nu = 30$ curve is somewhat steeper than that for $\nu = 0$. This is because of the broader barrier experienced at the higher frequency. Calculations for $T(\varepsilon)$ based upon the static effective potential were identical with those for ν values $\geqslant 30$, thus confirming the notion of a Born–Oppenheimer separation of timescales for particle and barrier motion.

Finally, and most interestingly, the transmission probability for a barrier of frequency $\nu = 5$ is shown in figure 3 and bears almost no resemblance to those for the high and low energy limits. Naively it might have been expected that this may lie

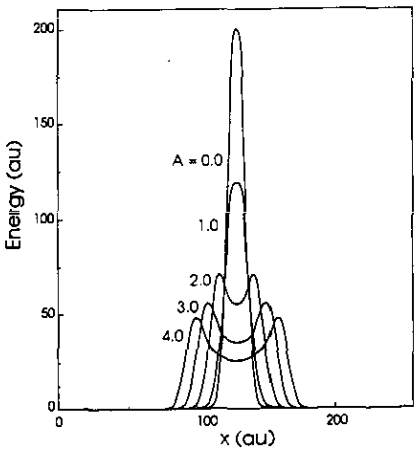

Figure 3. The time averaged potential (31) for a variety of amplitudes. When the period of the barrier is short, the particle cannot respond rapidly enough to changes. As a consequence the wavepacket interacts with a lower effective barrier (see figure 2).

between the $\nu = 0$ and 30 curves but this is definitely not the case. The results now become particularly dependent on the initial phase, ϕ, of the barrier and to illustrate this point, figure 4 shows the phase dependence of $T(\varepsilon)$ for ν values of 1, 2, 5 and 10 for an electron with energy 80 au. For $\nu = 1$, the results are almost ϕ-independent, similarly for $\nu = 12$. For $\nu = 2$, however, the transmission probability weakly depends upon ϕ varying between 0 and 0.1. For $\nu = 5$ this dependence has become strong with values ranging between 0.8 and 0.2 in a sinusoidal manner. The reason for the strong ϕ behaviour in the range $2 < \nu < 12$ is that a separation of timescales is now no longer valid and the outcome of the scattering event depends precisely upon the dynamics during the interaction. To investigate this in more detail, it is useful to examine the time dependence of the potenial and kinetic energies as the collision occurs.

Figure 5 shows the time dependence of the expectation values for the kinetic, potential and total energy during a collision of an electron with $\varepsilon = 80$ au on a stationary barrier. As the wavepacket begins to sample the barrier, kinetic energy is converted to potential energy until a time of ~75 au when the reflected particle moves out of the

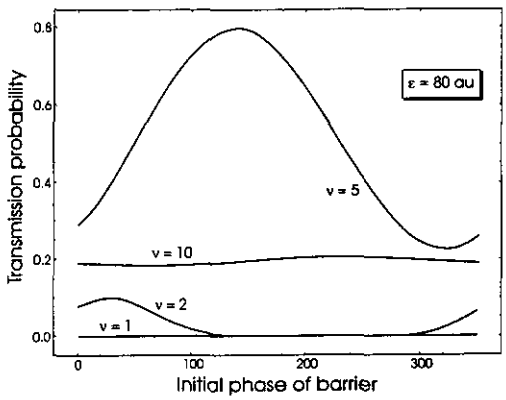

Figure 4. The transmission probability as a function of the initial phase for the oscillating position barrier. For low and high barrier frequencies, results are insensitive to the phase. When the period of the barrier and the particle interaction time are comparable ($\nu = 5$) there is a substantial dependence.

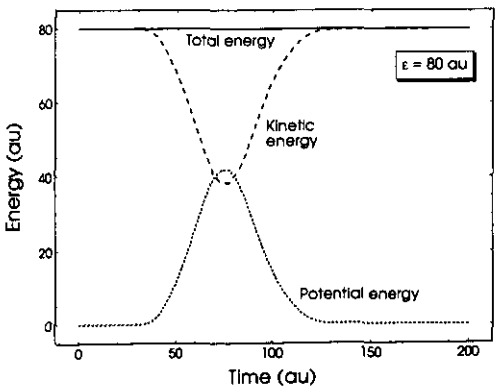

Figure 5. The time dependence of the expectation values of kinetic, potential and total energies for a wavepacket with energy 80 au striking a stationary Gaussian barrier of height 200 au.

region of interaction. For this case, energy is conserved and the transmission probability is zero.

Figures 6(a) and (b) show similar plots, but for the cases when $\nu = 2$ and $\phi = 200°$ and 30° which correspond to minima and maxima in $T(\varepsilon)$. In figure 6(a) there is an initial increase in potential energy at 50 au as the particle 'strikes' the barrier. Accompanying this, is a dramatic decrease in the kinetic energy which far outweighs the increase in potential. What is happening is that the particle suffers a collision with a receding barrier and almost comes to a halt. When the barrier returns, during the next cycle, the wavepacket is then reflected with a reduced energy of $\varepsilon = 30$ au. The collision is highly inelastic and the transmission probability is zero. In figure 6(b) there is only one peak in the potential energy curve implying a single 'strike'. As for the stationary barrier case, the kinetic energy falls as the collision occurs but with a modest phase lag with respect to the potential maximum. The particle strikes an approaching barrier which at the centre of its oscillation would imply, from (6), a relative kinetic energy of 179 au. This gives rise to a small tunnelling contribution of ~10% with a mean transmitted energy of 124 au. The reflected flux has also picked up momentum from the barrier and has a mean energy of 244 au.

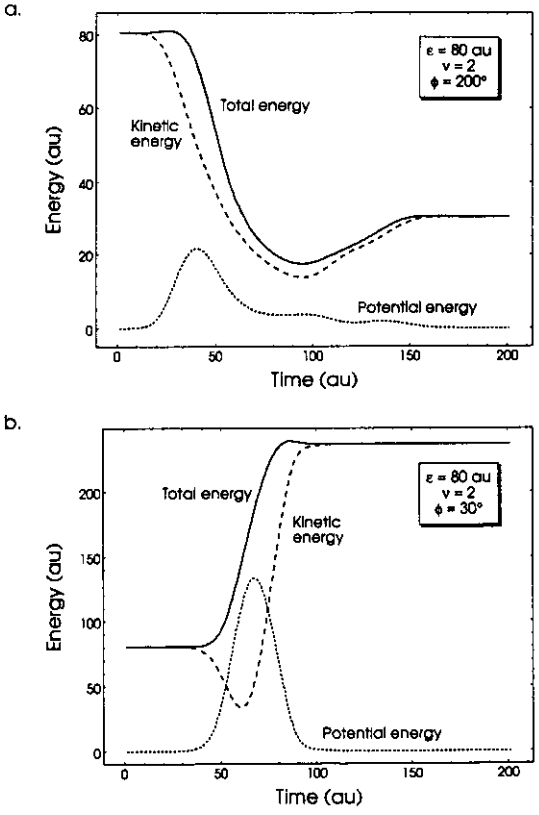

Figure 6. As figure 5 but for the case of an oscillating position barrier with frequency $\nu = 2$. In (a), at the time of the first collision, the barrier is moving away from the particle and hence the impact velocity is small. This results in a transfer of energy *to* the barrier and a low value of the transmission probability (figure 4). In (b), however, the particle and barrier are moving together at the time of the first collision resulting in a net energy *gain* by the particle and a higher transmission.

As the frequency is increased, more structure appears in these energy plots and an example, for $\nu = 5$ is shown in figure 7. Again phases corresponding to the maximum and minimum transmission probabilities have been chosen. Figure 7(a) shows the energies for an initial phase of 320° which corresponds to a transmission probability of 23%. The potential energy shows two peaks, each of which represents the wavepacket being struck by the barrier. For the initial encounter there is a significant drop in kinetic energy which this time is in phase with the increase in potential. This choice of phase results in an initial strike when the oscillator is moving towards the particle and between 5 and 10% tunnels at this time. The bulk of the packet is slowed up and after ~100 au it receives another impact which reflects ~77% and also produces a second pulse which tunnels through the barrier. The time delay between the two encounters corresponds to the period of the barrier. Again the overall collision is inelastic with the final mean energy ~120 au. For the case of maximum transmission, figure 7(b) is for an initial phase of 140° and has a simpler structure with only a single collision taking place. There is an initial encoutner after 25 au which is with a receding barrier and, as before, the particle is slowed up. In the next cycle the barrier passes right through the wavepacket, trapping a sizeable fraction (~77%) on the transmitted

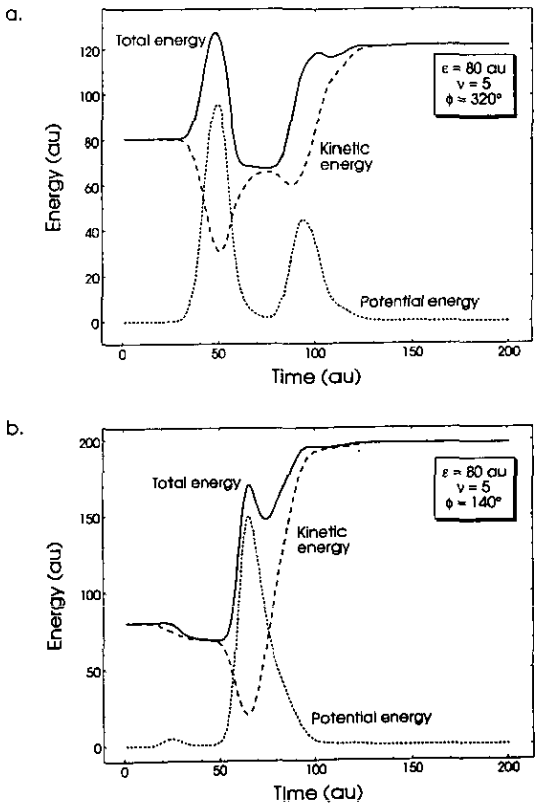

Figure 7. As figure 5 but for the case of an oscillating position barrier with frequency $\nu = 5$. Results are similar to those in figure 6 but now in both (a) and (b) the period of the barrier is short enough such that the particle suffers multiple interactions as evidence by the peaks in the potential energy profiles. See the text for a full description of both events.

side. This is a highly inelastic collision with the reflected and transmitted components having final mean energies of ~220 and 60 au respectively. As the frequency increases to even larger values, $T(\varepsilon)$ becomes independent of phase because there are so many collisions that the initial conditions are unimportant.

It is possible to average the transmission coefficient over the phase and figure 8 shows results for $\nu = 0$, 2, 5 and 15. For those frequencies in the range $2 \geqslant \nu \geqslant 12$, there are two main features in the $T(\varepsilon)$ curves to comment upon. At low energies ($\varepsilon < 100$ au) there is enhanced transmission over that obtained for frequencies lying above or below this range. This occurs because, for a range of phases, the barrier is moving towards the particle and thus the barrier appears to be lower. As shown above this effect is quite considerable and for an 80 au beam, can result in relative energies two and three times this value. The converse is seen for energies $\varepsilon > 200$ au, where the transmission probability is considerably lower than either the static or the high frequency result. This arises from those phases which have a barrier moving away from the wavepacket during the initial encounter, giving rise to a lowering of the translational energy and thereby reducing the transmission. This effect is seen quite clearly in the phase portraits shown in figure 4.

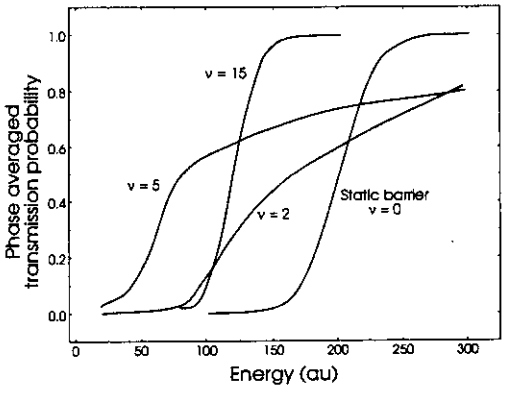

Figure 8. Transmission probability for a particle incident on an oscillating position barrier as a function of the initial translational energy. In this case the probabilities have been averaged over the initial phase of the barrier which makes a substantial difference only for the $\nu = 2$ and 5 cases. The enhancement at low energies is accounted for by collisions where the barrier and particle are moving together at the time of the initial impact.

Finally it is interesting to examine both the real and momentum space probability distributions during the scattering event to see if the conclusions presented in section 3 are borne out. In particular, it should be possible to trace the dynamic origins of the fine structure predicted in (14). Figure 9 shows a time-lapse sequence for a wavepacket with $\varepsilon = 200$ au striking a barrier oscillating with frequency 15. Both real and momentum space are shown and the times are indicated. The momentum space plots are perhaps the more revealing of the development of the collision. Starting with a sharp Gaussian at $t = 0$ a low energy tail begins to develop as the packet impinges on the barrier. In the central frames, the packet undergoes several strong collisions and a series of well defined peaks appear for positive momenta. The real space sequence shows that the packet is undergoing severe distortion as it traverses the barrier and a fine structure emerges for long times. Figure 10 shows a blow up of the asymptotic

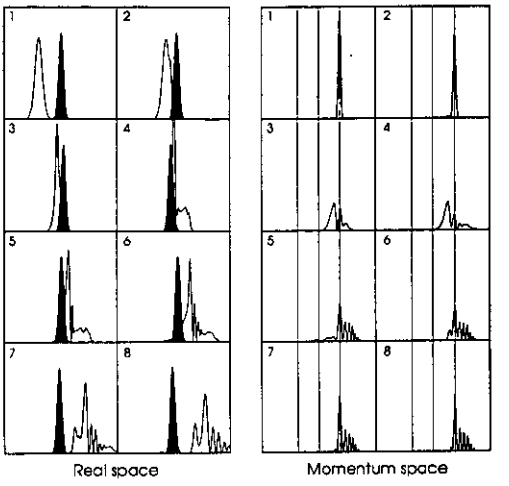

Figure 9. A time-lapse sequence for the scattering of a particle with energy 200 au from an oscillating position Gaussian barrier with height 200 au and frequency $\nu = 15$. The figure clearly shows the development of the fine structure in momentum space appearing in the transmitted flux. Frames are at a constant time interval of 0.066 au.

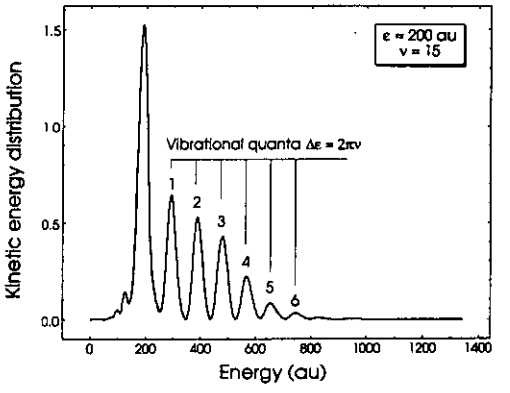

Figure 10. A blow up of the frame 8 momentum space distribution shown in figure 9. This has been re-plotted on an energy scale in order to show the equally separated satellites appearing to the high energy side of the elastically transmitted line. The energetic separation is $2\pi\nu$ au, the elementary excitation energy of the moving barrier.

transmitted packet plotted in energy rather than momentum space. This shows a very well resolved set of decaying peaks each separated by ω which is a manifestation of the superposition given in the wavefunction of (14). The number of quanta that have been excited is related to the length of time that the packet stays in the region of strong interaction which for the conditions in figure 10 is 9 cycles.

5.2. The oscillating amplitude barrier

Now we consider a potential of the form given by (1), a Gaussian barrier whose height is oscillating sinusoidally

$$V(x, t) = V_0(1 + A\sin(\omega t + \phi))\, e^{-\sigma[x-x_0]^2}. \tag{32}$$

Values for the constants were chosen to be those used above; $A = 0.5$ au, $V_0 = 200$ au and $\sigma = 1.0$ au. Again δ was chosen to be 0.5 au.

For the $\nu = 0$ limit of the oscillating barrier, the results are insensitive to ϕ since this simply acts to displace the origin of the packet. For the oscillating amplitude barrier there is a necessity to phase average even the $\nu = 0$ transmission probabilities since each value of ϕ defines a new potential. Figure 11 shows the phase averaged $T(\varepsilon)$ for frequencies of 0.5 and 15. In the high frequency limit, which again obtains for $\nu \geqslant 15$, $T(\varepsilon)$ is identical with the static barrier case. This is not a surprising result since by time averaging the potential defined by (32) one regains the static barrier of height V_0. Unlike the oscillating position barrier, there is a much weaker mechanism for increasing and decreasing the relative energy of the scattered particle with respect to the barrier, and the strong ϕ-dependence now arises because for some phases a judiciously low barrier is encountered. Figure 12 shows the phase dependence of the transmission probability for an energy of 200 au and frequencies 1, 2, 5 and 10.

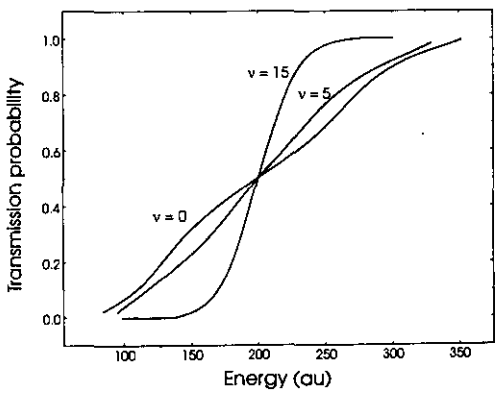

Figure 11. The phase averaged transmission probability for a particle incident on an oscillating amplitude barrier as a function of the initial translational energy. The barrier height is 200 au. This form of oscillation does not give rise to any Doppler shift in particle velocity and as such the results are less dramatic than those for the oscillating position barrier shown in figure 2.

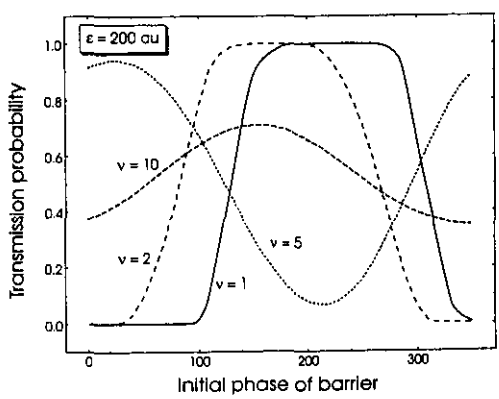

Figure 12. The phase dependence of a particle with 200 au energy on the oscillating amplitude barrier described in figure 11. The strong variation with the phase of the barrier simply arises from the distribution of barrier heights.

Interestingly enough the phase averaged value of $T(\varepsilon)$ for this case is independent of ν. While this is not a totally general result, calculated ν-dependences in the phase averaged $T(\varepsilon)$ tend to be weak. This is interesting because although momentum can be gained and lost in the scattering event, on average this does not drastically change the transmission probability.

6. Conclusions

We have presented a variety of solutions for the problem of a particle interacting with a moving barrier. It has been shown that depending upon whether the barrier amplitude or position oscillates, the solution to the classical problem is rather trivial but different for the two cases. Surprisingly the quantum solution appear remarkably similar. An exact solution has been found for the transmission coefficient for a plane wave incident on a spatially oscillating rectangular barrier. This problem is one that has been extensively studied in connection with the tunnelling time problem. Numerical simulations have been performed for a Gaussian wavepacket incident on a variety of oscillating barriers. In general, results show that there exist three distinct regions of solution depending upon the relative time scales of the particle velocity and the period of oscillation of the barrier. While the high and low frequency solutions are straightforward to understand in terms of static effective potential, when the two timescales are comparable then there exists a wide range of interesting dynamical effects.

Acknowledgments

It is a pleasure to acknowledge useful discussions with all members of the theory group in the Surface Science Research Centre, Liverpool. In addition A P thanks the British Council for partial support during his stay in Liverpool in the spring of 1989.

Appendix. Analytical approximations

In this appendix we investigate some semiclassical aspects of the time dependent barrier problem.

(*a*) *WKB Approximation for 1D time-dependent potentials*

Put the wavefunction in the form

$$\psi(x, t) = \exp[\mathrm{i}S(x, t)/\hbar] \tag{A1}$$

in the time-dependent Schrödinger equation. In the zeroth-order (terms independent of $\hbar$) we get the Hamilton–Jacobi equation for the action S:

$$\frac{1}{2m}\left(\frac{\partial S}{\partial x}\right)^2 + V(x, t) + \frac{\partial S}{\partial t} = 0. \tag{A2}$$

A simple way to solve (A2) is to consider a corresponding set of ordinary differential equations as shown, for example, by Courant and Hilbert [15]. With some algebra we

then obtain the following four equations:

$$dx/dt = p/m \tag{A3a}$$

$$dS/dt = p^2/m + q \tag{A3b}$$

$$dp/dt = -\partial V/\partial x \tag{A3c}$$

$$dq/dt = -\partial V/\partial t \tag{A3d}$$

where p, q are defined by

$$p \equiv \partial S/\partial x \qquad q \equiv \partial S/\partial t. \tag{A4a, b}$$

One integral of the system (A3) is directly given by the left-hand side of (A2) equal to a constant. Thus, to get the action, this constant must be set to zero, i.e.

$$p^2/2m + V(x, t) + q = 0. \tag{A5}$$

When the potential is independent of time, (A3d) is immediately integrated as

$$q = \text{constant} = -(p^2/2m + V) \equiv -E \tag{A6}$$

where E is the system energy. The action S is then readily obtained in the well known form

$$S(x, t) = \int^t L\, dt \tag{A7}$$

$$= -Et + \int^x dx\{2m[E - V(X)]\}^{1/2} \tag{A8}$$

where L is the Lagrangian

$$L = p^2/2m - V(x).$$

equation (A7) remains valid for time-dependent potentials, but its separation into space and time parts, as in (A8), is no more possible. Explicit calculation of S can be carried out in simple cases. The special situation

$$V(x, t) = V_0(x) + V_1(x, t)$$

where V_1 is 'small' in comparison with V_0 has been discussed by Zhang and Tzoar [6].

We now consider the case when the potential is of form (16). Making the coordinate transformation as in (18) and dropping the primes afterwards, equations (A3) become

$$dx/dt = p/m - f(t) \tag{A9a}$$

$$dS/dt = p^2/m + q \tag{A9b}$$

$$dp/dt = -dU/dx \tag{A9c}$$

$$dq/dt = f(t)\, dU/dx \tag{A9d}$$

where f is given by (19a). Solutions of (A9) satisfying the modified (A5), i.e.,

$$p^2/2m + U(x) + q = 0 \tag{A10}$$

give the action S (in primed coordinates). Eliminating p between (A9a) and (A9c) we get

$$m\, d^2x/dt^2 = -dU/dx - m\ddot{g}. \tag{A11}$$

Thus the motion in the moving reference frame corresponds to a conservative force due to potential U and an external force $-m\ddot{g}$. Integration of (A11) gives $x = x(t)$ which can be used in (A9c) to get $p(t)$; $q(t)$, then, is given by (A10) and quadrature of (A9b) would then give the action S.

(b) Eigenfunction expansion

We now consider an approximate way of solving the Schrödinger equation in moving coordinate frame given by (19). Assuming that $U(x)$ is Hermitian, let $\Phi_k(x)$ be a complete set of eigenfunctions satisfying

$$\frac{-\hbar^2}{2m}\frac{d^2\Phi_k}{dx^2} + U(x)\Phi_k(x) = E_k\Phi_k \tag{A12}$$

$$\langle\Phi_k|\Phi_{k'}\rangle = \delta_{kk'}. \tag{A12a}$$

We have assumed the index k to be discrete for simplicity; the continuum case can be readily dealt with in an analogous manner. Expand the wavefunction

$$\psi(x, t) = \sum_k C_k(t)\Phi_k(x) \tag{A13}$$

where the unknown coefficients $C_K(t)$ are to be obtained. Substitute (A13) in (19) and use (A12) and (A12a) to get

$$i\hbar\, dC_k/dt = C_kE_k - f(t)\sum_{k'} P_{kk'}C_{k'} \tag{A14}$$

where $P_{kk'}$ are the momentum matrix elements in the Φ_k representation:

$$P_{kk'} \equiv \int dx\, \Phi_k^*(x)(-i\hbar\,\partial/\partial x)\Phi_{k'}(x).$$

Equation (A14) can be written in the matrix form by introducing a column matrix $\tilde{C} = \{c_1 \ldots, c_k \ldots\}$, a diagonal matrix $\hat{E} = \text{diag}(E_1 \ldots, E_k \ldots)$ and the momentum matrix $\hat{P}$ with elements $P_{kk'}$ as

$$i\hbar\, d\tilde{C}/dt = [\hat{E} - f(t)\hat{P}]\tilde{C}. \tag{A15}$$

A formal solution of (A15) is readily obtained as

$$\tilde{C}(t) = \exp\left[\frac{i}{\hbar}(\hat{E}t - g(t)\hat{P})\right]\tilde{C}_0 \tag{A16}$$

where the constants in the column vector $\tilde{C}_0$ are to be chosen to satisfy the requisite initial conditions. Note that in general $\hat{E}$ and $\hat{P}$ do not commute. The form of (A16) shows that, with real $g(t)$, the wavefunction normalization does not change in time. Explicit calculations can be carried out using (A16) when the number of eigenfunctions involved in the expansion (A13) is restricted to a suitable finite number.

References

[1] Razavy M and Pimpale A 1988 *Phys. Rep.* **168** 305
[2] Büttiker M and Landauer R 1982 *Phys. Rev. Lett.* **49** 1793
[3] Büttiker M and Landauer R 1985 *Phys. Scr.* **32** 429
[4] Jauho A P and Jonson M 1989 *J. Phys.: Condens. Matter* 1 9027
[5] Hauge E H and Støvning J A 1989 *Rev. Mod. Phys.* **61** 917
[6] Zhang C and Tzoar N 1989 *Phys. Scr.* **T25** 333
[7] Holloway S 1990 *Interaction of Atoms and Molecules with Solid Surfaces* ed V Bortolani, N H March and M P Tosi (New York: Plenum) p 567

[8] Eastham M S P 1973 *The Spectral Theory of Periodic Differential Equations* (Edinburgh: Scottish Academic)
[9] Cutler P H, Feuchtwang T E, Huang Z, Tsong T T, Nguyen H, Lucas A A and Sullivan T E 1987 *J. Physique* **48C** 6-101
[10] Feit M D, Fleck J J A and Steiger A 1982 *J. Comput. Phys.* **47** 412
[11] Jackson B and Methiu H 1986 *J. Chem. Phys.* **86** 1026
[12] Halstead D and Holloway S 1988 *J. Chem. Phys.* **88** 717
[13] Hand M R and Holloway S 1989 *J. Chem. Phys.* **91** 7209
[14] Schiff L I 1968 *Quantum Mechanics* (New York: McGraw-Hill)
[15] Courant R and Hilbert D 1962 *Methods of Mathematical Physics* vol II (New York: Wiley)